

Dark matter contribution to $b \rightarrow s\mu^+\mu^-$ anomaly in local $U(1)_{L_\mu-L_\tau}$ model

Seungwon Baek

School of Physics, KIAS, Seoul 02455, Korea

E-mail: swbaek@kias.re.kr

ABSTRACT: We propose a local $U(1)_{L_\mu-L_\tau}$ model to explain $b \rightarrow s\mu^+\mu^-$ anomaly observed at the LHCb and Belle experiments. The model also has a natural dark matter candidate. We introduce colored $SU(2)_L$ -doublet scalar \tilde{q} to mediate $b \rightarrow s$ transition at one-loop level. The $U(1)_{L_\mu-L_\tau}$ is spontaneously broken by the scalar S . All the new particles are charged under $U(1)_{L_\mu-L_\tau}$. We can obtain $C_9^{\mu,\text{NP}} \sim -1$ to explain the $b \rightarrow s\mu^+\mu^-$ anomaly and explain the correct dark matter relic density of the universe, $\Omega_{\text{DM}}h^2 \approx 0.12$, while evading constraints from other FCNC processes such as $b \rightarrow s\gamma$ or $B_s - \overline{B}_s$ mixing. Our model can be tested by searching for new colored scalar at the LHC and $B \rightarrow K^*\nu\bar{\nu}$ process at Belle-II.

Contents

1	Introduction	1
2	The model	3
3	NP contribution to $b \rightarrow s$ transitions in our model	4
4	Dark matter relic density and direct detection	8
5	Conclusions	9
A	Loop functions	9

1 Introduction

Flavor changing neutral current (FCNC) processes are sensitive probe of new physics (NP) beyond the standard model (SM), of which the $b \rightarrow s\mu^+\mu^-$ has drawn much interest recently due to anomalies observed at the LHCb and Belle experiments. A form-factor independent angular observable P'_5 in the decay $B^0 \rightarrow K^{*0}\mu^+\mu^-$ shows 3.7σ discrepancy in the interval $4.3 < q^2 < 8.68 \text{ GeV}^2$, q^2 being dimuon invariant mass squared [1]. A global analysis of the CP-averaged angular observables indicates differences from the SM predictions at the level of 3.4σ [2]. These P'_5 anomaly has also been found by Belle collaborations at the level of $2.1 - 2.6\sigma$ [3, 4]. For the $B_s^0 \rightarrow \phi\mu^+\mu^-$ mode, the differential branching fraction has been found to be more than 3σ below the SM predictions in the range $1 < q^2 < 6 \text{ GeV}^2$ [5].

Most interesting observables are the ratios [6]

$$R_{K^{(*)}} \equiv \frac{\mathcal{B}(B \rightarrow K^{(*)}\mu^+\mu^-)}{\mathcal{B}(B \rightarrow K^{(*)}e^+e^-)}, \quad (1.1)$$

which are predicted to be $1 + O(m_\mu^2/m_b^2)$ representing the lepton-flavor universality (LFU) in the SM. They are theoretically very clean because the hadronic uncertainties are canceled in the ratios. The measured value R_K at LHCb in the range $1 < q^2 < 6 \text{ GeV}^2$ is $0.745^{+0.090}_{-0.074}(\text{stat}) \pm 0.036(\text{syst})$, deviating from the SM predictions by 2.6σ [7]. Recently the LHCb also measured R_{K^*} with the results [8].

$$R_{K^*} = \begin{cases} 0.66^{+0.11}_{-0.07}(\text{stat}) \pm 0.03(\text{syst}) & \text{for } 0.045 < q^2 < 1.1 \text{ GeV}^2, \\ 0.69^{+0.11}_{-0.07}(\text{stat}) \pm 0.05(\text{syst}) & \text{for } 1.1 < q^2 < 6.0 \text{ GeV}^2, \end{cases}$$

showing deviations at the level of $2.1 - 2.3\sigma$ and $2.4 - 2.5\sigma$ in the two q^2 regions, respectively.

It is worth noting that these possible deviations are in the same direction, and when combined, the discrepancy with the SM predictions is at the level of $\sim 5\sigma$ [9, 10]. The $b \rightarrow s\ell^+\ell^-$ decay is described by the effective weak Hamiltonian

$$\mathcal{H}_{\text{eff}} = -\frac{4G_F}{\sqrt{2}} V_{ts}^* V_{tb} \frac{e^2}{16\pi^2} \sum_i (C_i^\ell O_i^\ell + C_i'^\ell O_i'^\ell) + h.c., \quad (1.2)$$

where $O_i^{(\prime)}$'s are dimension 5 and 6 $b \rightarrow s$ transition operators, for example,

$$\begin{aligned} O_7 &= \frac{e^2}{16\pi^2} m_b (\bar{s}\sigma^{\mu\nu} P_R b) F_{\mu\nu}, & O'_7 &= \frac{e^2}{16\pi^2} m_b (\bar{s}\sigma^{\mu\nu} P_L b) F_{\mu\nu}, \\ O_9^\ell &= \frac{e^2}{16\pi^2} (\bar{s}\gamma_\mu P_L b) (\bar{\ell}\gamma^\mu \ell), & O_9'^\ell &= \frac{e^2}{16\pi^2} (\bar{s}\gamma_\mu P_R b) (\bar{\ell}\gamma^\mu \ell), \\ O_{10}^\ell &= \frac{e^2}{16\pi^2} (\bar{s}\gamma_\mu P_L b) (\bar{\ell}\gamma^\mu \gamma_5 \ell), & O_{10}'^\ell &= \frac{e^2}{16\pi^2} (\bar{s}\gamma_\mu P_R b) (\bar{\ell}\gamma^\mu \gamma_5 \ell). \end{aligned} \quad (1.3)$$

Writing $C_i^\ell = C_i^{\text{SM}} + C_i^{\text{NP}}$, the SM contribution at m_b scale is $C_7^{\text{SM}} \simeq -0.3$, $C_9^{\ell, \text{SM}} \simeq 4.2$, $C_{10}^{\ell, \text{SM}} \simeq -4.3$. The global fits to the experimental data show that the strongest ‘‘pull’’ is obtained in the scenario with NP in C_9 only [9]. The best fit value is $C_9^\mu = -1.21$ with pull 5.2σ .

There are already many works incorporating NP contribution to explain the violation of LFU in $b \rightarrow s\ell^+\ell^-$ decays with tree-level Z' contributions [11–28], with leptoquarks [29–36], and with loop-processes [37–42].

In this paper we propose a NP model with local $U(1)_{L_\mu-L_\tau}$ symmetry to solve the $b \rightarrow s\mu^+\mu^-$ anomaly. This model naturally breaks LFU between e and μ because the $U(1)_{L_\mu-L_\tau}$ gauge boson couples only to $\mu(\tau)$ but not to e . Many variants of $U(1)_{L_\mu-L_\tau}$ model have been studied previously: the Z' contribution to the muon ($g-2$) discrepancy [43], $U(1)_{L_\mu-L_\tau}$ -charged dark matter (DM) [44], predictions on neutrino parameters [45], very light Z' contribution to the annihilations of DM [46]. Especially the $U(1)_{L_\mu-L_\tau}$ model has also been extended to include to explain $b \rightarrow s\mu^+\mu^-$ anomaly, but in different context from our model [47–49]. Our model has $U(1)_{L_\mu-L_\tau}$ -charged colored scalars which we call *squark* coupling to s, b -quarks, while the ref. [47] introduces vector-like quarks. The former has one-loop contribution to $b \rightarrow s\mu^+\mu^-$, whereas the latter has tree-leve contribution. Our model has also a natural dark matter candidate. It corresponds to the scenario with NP in C_9 only mentioned above, which is obtained from the Z' -penguin diagrams. There is no box-diagram contribution at one-loop level. In our model C_9 includes contribution from $b \rightarrow s$ transition which comes from quark-squark-DM Yukawa interaction as well as contribution from $U(1)_{L_\mu-L_\tau}$ gauge interactions. The $b \rightarrow s$ transition part is strongly constrained by other quark FCNC processes such as $b \rightarrow s\gamma$ and $B_s - \bar{B}_s$, which can be evaded easily in our scenario.

The paper is organized as follows. In section 2, we introduce our model. The section 3 presents the results for NP contributions to $b \rightarrow s\mu^+\mu^-$, $b \rightarrow s\gamma$, and $B_s - \bar{B}_s$ mixing and shows that we can accommodate both $b \rightarrow s\mu^+\mu^-$ anomaly and the correct relic density of the universe. In the section 4 we discuss DM phenomenology. We conclude in section 5.

2 The model

We introduce a local $U(1)_{L_\mu-L_\tau}$ symmetry in addition to the SM gauge group. The second (third) generation left-handed lepton doublet and right-handed singlet, $\ell_L^\mu, \mu_R, (\ell_L^\tau, \mu_R)$, are charged under $U(1)_{L_\mu-L_\tau}$ with charge 1(−1). It is a well-known fact that the $U(1)_{L_\mu-L_\tau}$ is anomaly-free even without extending the SM particle content. We also introduce new particles which are charged under $U(1)_{L_\mu-L_\tau}$, a Dirac fermion N , a colored $SU(2)_L$ -doublet scalar $\tilde{q} \equiv (\tilde{u}, \tilde{d})^T$, and a singlet-scalar S . Since the new fermion N is a Dirac particle, the theory is free from gauge anomaly. Their charge assignments are shown in Table 1.

	New fermion	New scalars	
	N	\tilde{q}	S
$SU(3)_C$	1	3	1
$SU(2)_L$	1	2	1
$U(1)_Y$	0	$\frac{1}{6}$	0
$U(1)_{L_\mu-L_\tau}$	Q	$-Q$	$2Q$

Table 1. Charge assignments of N, \tilde{q} and S under the SM gauge group and $U(1)_{L_\mu-L_\tau}$. We take $Q \neq 0, \pm 1$.

The Lagrangian is written as

$$\begin{aligned} \mathcal{L} = & \mathcal{L}_{\text{SM}} - V - \frac{1}{4} Z'_{\mu\nu} Z'^{\mu\nu} + \overline{N} (i\gamma^\mu D_\mu - M_N) N + (D_\mu \tilde{q}^\dagger) (D^\mu \tilde{q}) - m_{\tilde{q}}^2 \tilde{q}^\dagger \tilde{q} \\ & + (D_\mu S^\dagger) (D^\mu S) - m_S^2 S^\dagger S - \sum_{i=s,b} (y_L^i \overline{q}_L^i \tilde{q} N + h.c.) - \left(\frac{f}{2} \overline{N^c} N S^\dagger + h.c. \right), \end{aligned} \quad (2.1)$$

where $Z'_{\mu\nu} \equiv \partial_\mu Z'_\nu - \partial_\nu Z'_\mu$ is field strength tensor for $U(1)_{L_\mu-L_\tau}$ gauge boson Z' , and D_μ is the covariant derivative. The N^c is the charge conjugate state of N . The scalar potential V including the SM Higgs parts can be written as

$$V = -\mu_H H^\dagger H - \mu_S S^\dagger S + \lambda_H (H^\dagger H)^2 + \lambda_S (S^\dagger S)^2 + \lambda_{HS} (H^\dagger H)(S^\dagger S), \quad (2.2)$$

where H is the SM Higgs doublet. The field \tilde{q} and N mediate the $U(1)_{L_\mu-L_\tau}$ interaction to quark sector. Although $i = d$ is allowed by the gauge symmetry in general, we neglect the interaction with down-quark in this paper, because it is irrelevant in our discussion of $b \rightarrow s\ell\ell$ transition. We assume the q 's are already in the mass eigenstates so that there is no further flavor mixing due to CKM mixing. The flavored-DM scenarios have been also studied in [16, 50–52]. Since N and N^c are mixed, they are not mass eigenstates. The mass matrix of N and N^c is written as

$$\begin{pmatrix} M_N & \frac{f v_S}{\sqrt{2}} \\ \frac{f v_S}{\sqrt{2}} & M_N \end{pmatrix}, \quad (2.3)$$

where v_S is vacuum expectation value (VEV) of S , $\langle S \rangle = v_S/\sqrt{2}$. The mass eigenstates are mixture of N and N^c ,

$$\begin{aligned} N_- &= \frac{1}{\sqrt{2}}(N - N^c), \\ N_+ &= \frac{1}{\sqrt{2}}(N + N^c), \end{aligned} \quad (2.4)$$

whose masses are $m_{\mp} = M_N \mp fv_S/\sqrt{2}$. The N_{\mp} are two Majorana particles. The N_- state has Majorana phase π so that $N_-^c = -N_-$, but $N_+^c = N_+$. In the unitary gauge, S can be decomposed as $S = 1/\sqrt{2}(v_S + \phi_S)$. The real scalar ϕ_S can also mix with the SM Higgs boson h via λ_{HS} term in (2.2). The mixing angle is denoted as α_H . The mixing parameter is constrained by the LHC experiments. The details can be found in [53, 54]. In this work, the mixing between ϕ_S and h does not affect $b \rightarrow s\mu^+\mu^-$, but it affects the dark matter phenomenology. The direct detection experiments of dark matter strongly constrains this *Higgs portal interaction*. Therefore we take $\alpha_H = 0.001$ in our numerical analysis to evade the constraints from LHC and DM direct detection experiments.

After $U(1)_{L_\mu-L_\tau}$ is broken by the VEV of S , v_S , there is still remnant Z_2 symmetry due to the last terms in (2.1). This discrete symmetry stabilizes the lightest neutral Z_2 odd particle, which we assume is N_- . And it becomes a good dark matter candidate. As mentioned above the DM interacts with the SM sector mediated either by the Higgs portal or Z' . The DM pair annihilates through $N_-N_- \rightarrow Z'Z'$ or coannihilation process $N_-N_+ \rightarrow Z' \rightarrow \mu^+\mu^-(\tau^+\tau^-)$ in case the mass difference $\Delta m \equiv m_+ - m_- = \sqrt{2}fv_S$ is small. There is also annihilation into the SM particles through the ϕ_S and the SM Higgs mixing (Higgs portal). Notice that we take the $U(1)_{L_\mu-L_\tau}$ charge of N , $Q \neq 0, \pm 1$, so that the Yukawa interactions $\overline{\ell}_L^\mu \tilde{H} N$ and $\overline{\ell}_L^\tau \tilde{H} N$ are *not* allowed. Otherwise N can mix with the active neutrinos, ν_μ or ν_τ , and N cannot be the electroweak scale WIMP DM candidate.

After S gets VEV, the $U(1)_{L_\mu-L_\tau}$ gauge boson gets mass, $m_{Z'} = 2g_X|Q|v_S$, where g_X is the $U(1)_{L_\mu-L_\tau}$ gauge coupling constant. The colored-scalars \tilde{u} and \tilde{d} have degenerate mass $m_{\tilde{q}}$ at tree-level. The mass splitting occurs via isospin breaking electroweak interactions. For our purpose, we need just the mass of $m_{\tilde{d}}$, which we take $m_{\tilde{d}} = m_{\tilde{q}}$.

3 NP contribution to $b \rightarrow s$ transitions in our model

In our model the $b \rightarrow s\mu^+\mu^-$ transition operator O_9^μ is generated by Z' -exchanging penguin diagrams as shown in Fig. 1. From the diagrams we can see that only $C_9^{\mu(\tau),\text{NP}}$ is generated. There is no box diagram contribution at one-loop level. The result is

$$C_9^{\mu,\text{NP}} = -Q \frac{\sqrt{2}}{4G_F m_{Z'}^2} \frac{\alpha_X}{\alpha_{\text{em}}} \frac{y_L^s y_L^b}{V_{ts}^* V_{tb}} \mathcal{V}_{sb}(x_-, x_+), \quad (3.1)$$

where $\alpha_X = g_X^2/(4\pi)$, $x_{\mp} = m_{\mp}^2/m_{\tilde{d}}^2$, and $\mathcal{V}_{tb}(x_-, x_+)$ is the effective $b - s - Z'$ vertex at zero momentum transfer. The expression for \mathcal{V}_{sb} is given in the appendix A. In the limit $m_- = m_+$ we obtain $\mathcal{V}_{sb}(x_-, x_-) = 0$. This can be understood from the fact we took zero momentum limit to get \mathcal{V}_{sb} . In the limit $m_- = m_+$, the two Majorana fermions N_{\mp} return

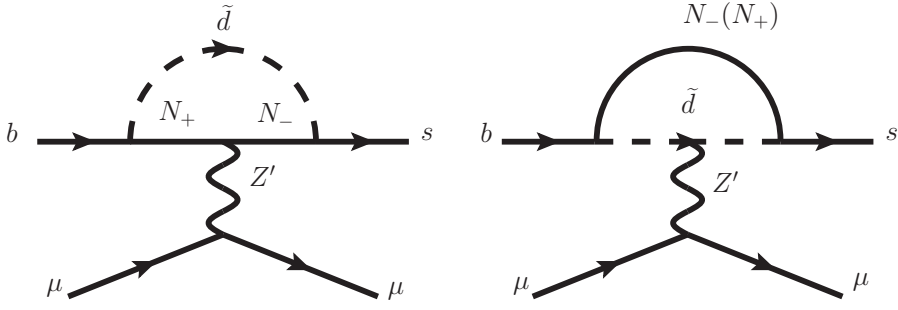


Figure 1. Penguin diagrams generating $b \rightarrow s\mu^+\mu^-$ in our model.

to the original Dirac fermion N . And the $U(1)_{L_\mu - L_\tau}$ gauge symmetry is restored, and $\mathcal{V}_{sb}(x_-, x_-) = 0$ is simply a consequence of gauge invariance. Therefore, to get a sizable $C_9^{\mu, \text{NP}}$ we need large mass splitting Δm , which implies the dominance of DM coannihilation processes for the DM relic and large $C_9^{\mu, \text{NP}}$ are not compatible in our scenario. Fig. 2 shows a contour plot for $C_9^{\mu, \text{NP}}$ (black lines) in the plane (x_-, x_+) . For the plot we fixed $Q = 3/2$, $\alpha_X = 0.2$, $y_L^s y_L^b = 0.01$, $m_{Z'} = 300$ GeV, and $m_{\tilde{d}} = 1$ TeV. In the same plot we also show $\Omega h^2 = 0.12$ lines (red lines), which could explain the DM relic in the universe. The DM phenomenology will be discussed in more detail in Section 4. We can see that $C_9^{\mu, \text{NP}} \sim -1$ can be obtained with sizable mass splittings, which can explain the $b \rightarrow s\mu^+\mu^-$ anomaly. We also note that the value of $C_9^{\mu, \text{NP}}$ does not depend on the absolute value of $m_{\tilde{d}}$ or $m_{\tilde{\tau}}$ but only on their ratios. We take $m_{\tilde{d}} = 1$ TeV as a reference value, which is needed for DM phenomenology and other FCNC processes, $b \rightarrow s\gamma$ and $B_s - \overline{B}_s$ mixing.

The couplings y_L^s and y_L^b also generate other quark FCNC processes such as $b \rightarrow s\gamma$ and $B_s - \overline{B}_s$ mixing. The experimental measurement of the inclusive branching fraction of radiative B -decay, $\overline{B} \rightarrow X_s \gamma$, is [55]

$$\mathcal{B} \left[\overline{B} \rightarrow X_s \gamma, \left(E_\gamma > \frac{1}{20} m_b \right) \right]^{\text{exp}} = (3.32 \pm 0.15) \times 10^{-4}, \quad (3.2)$$

which can be compared with theoretical prediction in the SM [56],

$$\mathcal{B} \left[\overline{B} \rightarrow X_s \gamma, (E_\gamma > 1.6 \text{ GeV}) \right]^{\text{SM}} = (3.57 \pm 0.30) \times 10^{-4}. \quad (3.3)$$

The NP contribution to C_7^γ at the electroweak scale whose diagram is shown in Fig. 3 is obtained to be

$$C_7^{\gamma, \text{NP}} = -\frac{\sqrt{2} e_d}{16 G_F m_{\tilde{d}}^2} \frac{y_L^s y_L^b}{V_{ts}^* V_{tb}} [J_1(x_-) + J_1(x_+)], \quad (3.4)$$

where $e_d = -1/3$, and the loop function $J_1(x)$ is given in the Appendix A. The corresponding SM value is $C_7^{\gamma, \text{SM}}(\mu_b) \approx -0.3$ [57].

The NP contribution to $B_s - \overline{B}_s$ mixing occurs via the box diagrams shown in Fig. 4. The mass difference in the $B_s - \overline{B}_s$ system has been measured by CDF and LHCb and the

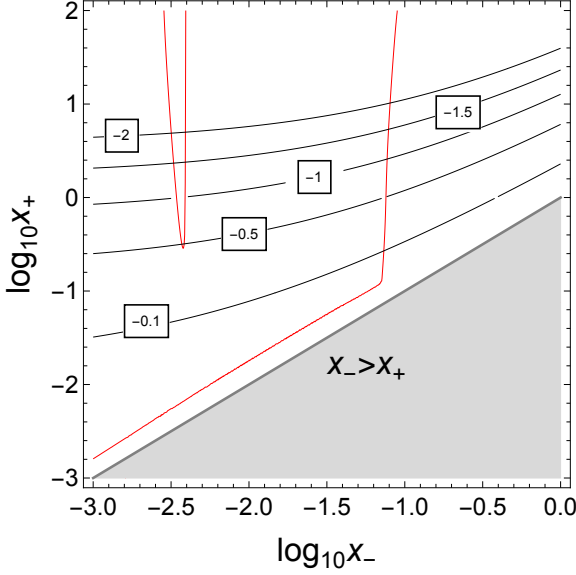


Figure 2. Contour plot for $C_9^{\mu, \text{NP}}$ at the electroweak scale (black lines) and $\Omega h^2 = 0.12$ (red lines) in the plane (x_-, x_+) . We fixed $Q = 3/2$, $\alpha_X = 0.2$, $y_L^s y_L^b = 0.01$, $m_{Z'} = 300$ GeV, and $m_{\tilde{d}} = 1$ TeV. We also take $m_{H_2} = 1$ TeV and $\alpha_H = 0.001$.

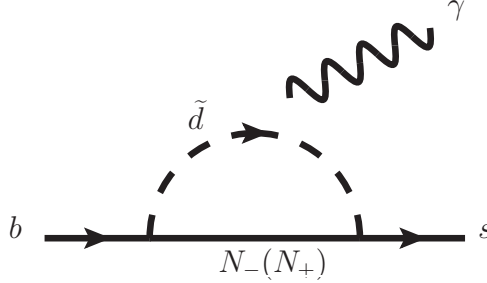


Figure 3. Feynman diagrams for $b \rightarrow s\gamma$ in our model. The photon can be attached to electrically charged particles, \tilde{d}, b or s .

average value is

$$\Delta m_s = 17.757 \pm 0.020(\text{stat}) \pm 0.007(\text{syst}) \text{ ps}^{-1}, \quad (3.5)$$

which is in good agreement with the SM predictions [58] with predictions 17.5 ± 1.1 ps $^{-1}$ [59] or $16.73^{+0.82}_{-0.57}$ ps $^{-1}$ [60]. More recently the ref. [61] reports larger central value for the SM prediction but with larger errors, $\Delta m_s^{\text{SM}} = 18.6^{+2.4}_{-2.3}$. The effective Hamiltonian in the SM has $(V - A) \times (V - A)$ structure since the W -boson couples only to left-handed quarks,

$$\mathcal{H}_{\text{eff}}^{\Delta B=2} = \frac{G_F m_W^2}{4\pi^2} (V_{ts}^* V_{tb})^2 S_0(x_t) \bar{s} \gamma_\mu P_L b \bar{s} \gamma^\mu P_L b \equiv C_1^{\text{SM}}(\mu_W) \bar{s} \gamma_\mu P_L b \bar{s} \gamma^\mu P_L b, \quad (3.6)$$

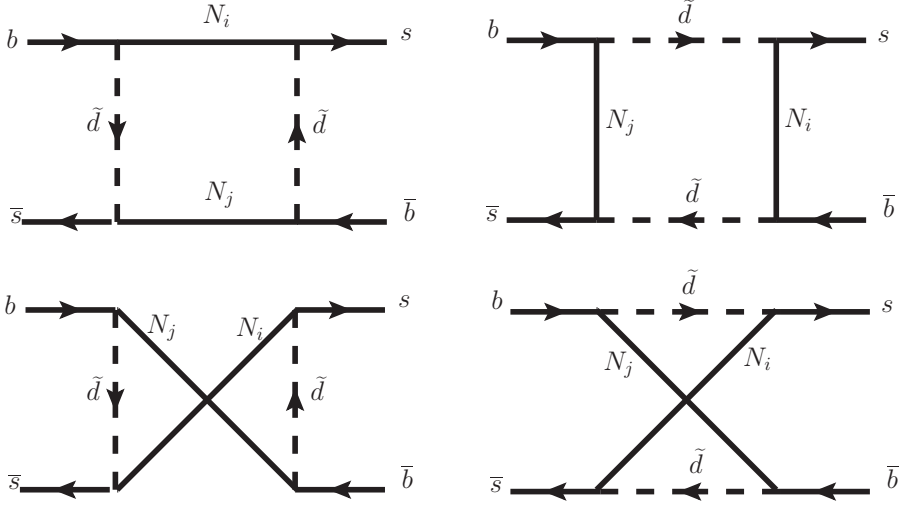


Figure 4. Box diagrams which contribute to $B_s - \bar{B}_s$ mixing, where $i, j = \pm$.

where $x_t = m_t^2/m_W^2$ and the loop function $S_0(x_t)$ can be found, *e.g.*, in [57]. The NP contribution to the $B_s - \bar{B}_s$ mixing whose Feynman diagrams are shown in Fig. 4 can also be written in the form

$$\mathcal{H}_{\text{eff}}^{\Delta B=2, \text{NP}} = C_1^{\text{NP}} \bar{s} \gamma_\mu P_L b \bar{s} \gamma^\mu P_L b, \quad (3.7)$$

where at the electroweak scale

$$C_1^{\text{NP}}(\mu_W) = \frac{(y_L^s y_L^b)^2}{128\pi^2 m_d^2} \left[2k(x_-, x_-, 1) + 4k(x_-, x_+, 1) + 2k(x_+, x_+, 1) + x_- j(x_-, x_-, 1) + 2\sqrt{x_- x_+} j(x_-, x_+, 1) + x_+ j(x_+, x_-, 1) \right], \quad (3.8)$$

where the loop functions j and k are listed in the Appendix A. Since new particles in our model couple only to the left-handed quarks as shown in (2.1), the NP operator has the same Lorentz structure with the SM operator in (3.6).

By comparing the experimental results and the SM predictions, we can see that both $b \rightarrow s\gamma$ and $B_s - \bar{B}_s$ mixing still allows $\sim 10\%$ contribution from NP. To see the impact of these FCNC constraints on our model, we show contour plots for $C_7^{\gamma, \text{NP}}/C_7^{\gamma, \text{SM}}$ for $b \rightarrow s\gamma$ and $C_1^{\text{NP}}/C_1^{\text{SM}}$ for $B_s - \bar{B}_s$ mixing at the electroweak scale. We take the same parameters with Fig. 2. We see the NP contribution to the $b \rightarrow s\gamma$ is typically a few $\times O(10^{-4})$ of the SM contribution and its contribution to the $B_s - \bar{B}_s$ mixing is at most $\lesssim 1\%$. Consequently we can safely evade the constraints for the parameters chosen in Fig. 2. We also checked even for the relatively large $\Delta m = \sqrt{2} f v_S$, the dark Yukawa coupling f can be still in the perturbative regime, *i.e.* $f \lesssim 4\pi$. The key observation is that the large contribution to $C_9^{\mu, \text{NP}}$ comes from the relatively light Z' ($m_{Z'} \sim O(100)$ GeV) and sizable $U(1)_{L_\mu - L_\tau}$ coupling, $\alpha_X \sim 0.1 - 1$, while Z' gauge boson is not involved in $b \rightarrow s\gamma$ or $B_s - \bar{B}_s$ mixing at the one-loop level.

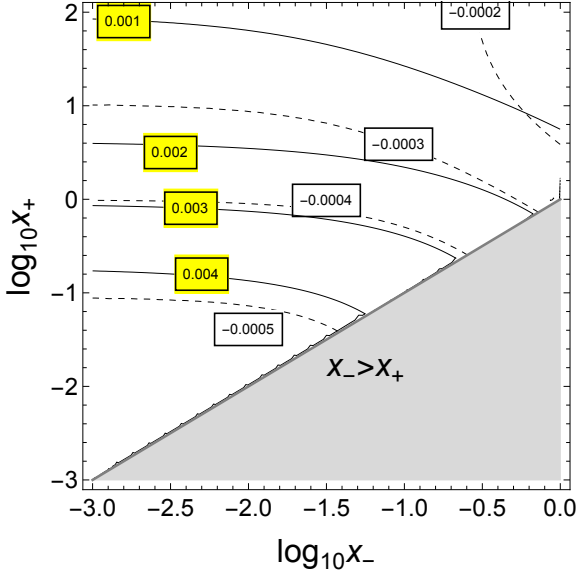


Figure 5. Contour plots for $C_7^{\gamma, \text{NP}}/C_7^{\gamma, \text{SM}}$ (dashed lines) and $C_1^{\text{NP}}/C_1^{\text{SM}}$ (solid lines) at the electroweak scale. The fixed parameters are the same with Fig. 2.

4 Dark matter relic density and direct detection

There are many DM annihilation diagrams for the relic density in our model: $H_1(H_2)$ -mediated s -channel diagrams for $N_- N_- \rightarrow \text{SM}, \text{SM}$ (Higgs portal contributions), \tilde{d} -mediated t -channel diagrams for $N_- N_- \rightarrow ss, sb, bb$, and $N_- N_- \rightarrow Z'Z'$ which have both Higgs-mediated s -channel and N_+ -mediated t -channel diagrams. Also coannihilation diagrams can make contributions when $\Delta m (= m_+ - m_-)$ is small compared to m_- . But when coannihilation dominates, it is difficult to get sizable $C_9^{\mu, \text{NP}}$, which can be seen also in Fig. 2.

Fig. 2 shows contour lines for the total DM relic density $\Omega_{\text{DM}} h^2 \approx 0.12$ (red lines). The lines intersect with the contour line with $C_9^{\mu, \text{NP}} \sim -1$. And we can accommodate both the $R_{K^{(*)}}$ anomaly and the correct DM relic density of the universe in our model. To calculate the relic density we implemented our model to the numerical package micrOMEGAs [62]. The Higgs portal contribution is controlled by the Higgs-mixing parameter α_H [53]. Since α_H is strongly constrained both by the searches for Higgs invisible decays at the LHC and by the DM direct search experiments, we fix it to be small, $\alpha_H = 0.001$. But still we can see the SM-Higgs resonance diagram can saturate $\Omega_{\text{DM}} h^2 \simeq 0.12$ in Fig. 2 near $\log_{10} x_- \approx -2.5$ (*i.e.* $m_- \approx 63$ GeV for $m_{\tilde{d}} = 1$ TeV). We can also see the coannihilation region near $x_+ = x_-$ line. But this coannihilation region is not favored by the $b \rightarrow s\mu^+\mu^-$ anomaly as stated above. The noble and the most interesting contributions in our scenario are $N_- N_- \rightarrow Z'Z'$ modes (almost vertical part of red line near $x_- = 1.2$). To obtain contribution to $C_9^{\mu, \text{NP}}$ with the size that can explain the $b \rightarrow s\mu^+\mu^-$ anomaly, we need relatively light Z' and sizable α_X . When the mode is kinematically open, it can give large cross section enough to explain the correct relic density of the universe.

Once we take small α_H , the tree-level Higgs contribution to the DM scattering cross

section with nucleons are suppressed below the current bounds. Although new particles can contribute to the direct DM searches, the diagrams first occur at one-loop level, so they are loop-suppressed. Since we take heavy $m_{\tilde{d}} (\approx 1 \text{ TeV})$ we expect the loop contribution is not large enough to saturate the current bound and we do not calculate the cross section in this paper.

5 Conclusions

The LHCb and Belle experiments have observed anomaly in $b \rightarrow s\mu^+\mu^-$ processes in the observables of P'_5 , $R_{K^{(*)}}$ and $\mathcal{B}(B_s^0 \rightarrow \phi\mu^+\mu^-)$. The global fits show $\sim 5\sigma$ deviation from the standard model predictions with the best fit value $C_9^{\mu, \text{NP}} \sim -1$ for $C_9^{\mu, \text{NP}}$ only scenario. We propose a local $U(1)_{L_\mu - L_\tau}$ model which can explain the $b \rightarrow s\mu^+\mu^-$ anomaly. The model also contains a natural dark matter candidate. The new physics contribution to $b \rightarrow s$ transition occurs via the exchange of colored $SU(2)_L$ -doublet scalar \tilde{q} which is also charged under $U(1)_{L_\mu - L_\tau}$. To conserve $U(1)_{L_\mu - L_\tau}$ charge in the Yukawa interaction of \tilde{q} with the SM quarks b, s , we need a Dirac fermion N which is electrically neutral but charged under $U(1)_{L_\mu - L_\tau}$ so that the Yukawa interaction takes the form $y_L^i \tilde{q}_L^i \tilde{q} N + h.c.$. The stability of dark matter candidate N is achieved by the interaction $f \overline{N^c} N S^\dagger + h.c.$ where S is $U(1)_{L_\mu - L_\tau}$ -breaking scalar, which leaves exact Z_2 symmetry after S obtains vacuum expectation value. The lightest Z_2 -odd neutral Majorana fermion mass eigenstate N_- becomes a stable dark matter candidate.

The model contributes to the C_9^μ for $b \rightarrow s\mu^+\mu^-$ through the Z' -exchanging penguin diagrams. When $\alpha_X \sim 0.2$, $m_{Z'} \sim 300 \text{ GeV}$, we can explain the $R_{K^{(*)}}$ anomaly since our Z' does not couple to electrons but to muons, resulting in the violation of lepton flavor universality. Large mass splitting between N_\pm states are favored for large $C_9^{\mu, \text{NP}}$. The constraints on $b \rightarrow s$ transition from $b \rightarrow s\gamma$ and $B_s - \overline{B}_s$ mixing can be evaded by taking relatively heavy ($\sim 1 \text{ TeV}$) \tilde{q} and small product of Yukawa couplings, $y_L^s y_L^b \sim 0.01$.

Our dark matter can provide the correct relic density via the annihilations of the Higgs resonance channel and $N_- N_- \rightarrow Z' Z'$ channel. The latter channel is naturally realized in our model because Z' is relatively light and has sizable gauge coupling with the dark fermions N_\pm . Our model can be tested by searching for new colored scalar at the LHC and $B \rightarrow K^* \nu \bar{\nu}$ process at Belle-II.

A Loop functions

The effective $b - s - Z'$ vertex at zero momentum transfer is given by the loop function at zero momentum transfer,

$$\mathcal{V}_{sb}(x_-, x_+) = \frac{1}{4} + \frac{\sqrt{x_- x_+}(f_1(x_-) - f_1(x_+))}{x_- - x_+} - \frac{f_2(x_-) - f_2(x_+)}{2(x_- - x_+)} + I(x_-) + I(x_+), \quad (\text{A.1})$$

where $x_{\mp} = m_{\mp}^2/m_d^2$ and

$$\begin{aligned} j(x) &= \frac{x \log x}{x-1}, \\ k(x) &= \frac{x^2 \log x}{x-1}, \\ I(x) &= \frac{-3x^2 + 4x - 1 + 2x^2 \log x}{8(x-1)^2}. \end{aligned} \quad (\text{A.2})$$

The loop function $J_1(x)$ for $b \rightarrow s\gamma$ is obtained to be

$$J_1(x) = \frac{1 - 6x + 3x^2 + 2x^3 - 6x^2 \log x}{12(1-x)^4}. \quad (\text{A.3})$$

The loop functions for the $\Delta B = 2$ box diagrams can be obtained from the functions in (A.2), $j(x)$ and $k(x)$. The functions with more than one argument are defined recursively as

$$f(x_1, x_2, x_3, \dots) \equiv \frac{f(x_1, x_3, \dots) - f(x_2, x_3, \dots)}{x_1 - x_2}, \quad (\text{A.4})$$

for each function $f = j, k$.

Acknowledgments

The author is grateful to Yuji Omura, Jusak Tandean and Chaehyun Yu for useful discussions. This work is supported in part by National Research Foundation of Korea (NRF) Research Grant NRF-2015R1A2A1A05001869.

References

- [1] LHCb collaboration, R. Aaij et al., *Measurement of Form-Factor-Independent Observables in the Decay $B^0 \rightarrow K^{*0} \mu^+ \mu^-$* , *Phys. Rev. Lett.* **111** (2013) 191801, [[1308.1707](#)].
- [2] LHCb collaboration, R. Aaij et al., *Angular analysis of the $B^0 \rightarrow K^{*0} \mu^+ \mu^-$ decay using 3 fb^{-1} of integrated luminosity*, *JHEP* **02** (2016) 104, [[1512.04442](#)].
- [3] BELLE collaboration, A. Abdesselam et al., *Angular analysis of $B^0 \rightarrow K^*(892)^0 \ell^+ \ell^-$, in Proceedings, LHCSci 2016 - A First Discussion of 13 TeV Results: Obergurgl, Austria, April 10-15, 2016*, [1604.04042](#).
- [4] BELLE collaboration, S. Wehle et al., *Lepton-Flavor-Dependent Angular Analysis of $B \rightarrow K^* \ell^+ \ell^-$* , *Phys. Rev. Lett.* **118** (2017) 111801, [[1612.05014](#)].
- [5] LHCb collaboration, R. Aaij et al., *Angular analysis and differential branching fraction of the decay $B_s^0 \rightarrow \phi \mu^+ \mu^-$* , *JHEP* **09** (2015) 179, [[1506.08777](#)].
- [6] G. Hiller and F. Kruger, *More model-independent analysis of $b \rightarrow s$ processes*, *Phys. Rev. D* **69** (2004) 074020, [[hep-ph/0310219](#)].
- [7] LHCb collaboration, R. Aaij et al., *Test of lepton universality using $B^+ \rightarrow K^+ \ell^+ \ell^-$ decays*, *Phys. Rev. Lett.* **113** (2014) 151601, [[1406.6482](#)].

[8] LHCb collaboration, R. Aaij et al., *Test of lepton universality with $B^0 \rightarrow K^{*0} \ell^+ \ell^-$ decays*, [1705.05802](#).

[9] W. Altmannshofer, C. Niehoff, P. Stangl and D. M. Straub, *Status of the $B \rightarrow K^* \mu^+ \mu^-$ anomaly after Moriond 2017*, *Eur. Phys. J. C* **77** (2017) 377, [[1703.09189](#)].

[10] B. Capdevila, A. Crivellin, S. Descotes-Genon, J. Matias and J. Virto, *Patterns of New Physics in $b \rightarrow s \ell^+ \ell^-$ transitions in the light of recent data*, [1704.05340](#).

[11] Q. Chang, X.-Q. Li and Y.-D. Yang, *A comprehensive analysis of hadronic $b \rightarrow s$ transitions in a family non-universal Z-prime model*, *J. Phys. G* **41** (2014) 105002, [[1312.1302](#)].

[12] A. Crivellin, G. D'Ambrosio and J. Heeck, *Addressing the LHC flavor anomalies with horizontal gauge symmetries*, *Phys. Rev. D* **91** (2015) 075006, [[1503.03477](#)].

[13] B. Allanach, F. S. Queiroz, A. Strumia and S. Sun, *Z models for the LHCb and $g - 2$ muon anomalies*, *Phys. Rev. D* **93** (2016) 055045, [[1511.07447](#)].

[14] S. M. Boucenna, A. Celis, J. Fuentes-Martin, A. Vicente and J. Virto, *Non-abelian gauge extensions for B-decay anomalies*, *Phys. Lett. B* **760** (2016) 214–219, [[1604.03088](#)].

[15] S. M. Boucenna, A. Celis, J. Fuentes-Martin, A. Vicente and J. Virto, *Phenomenology of an $SU(2) \times SU(2) \times U(1)$ model with lepton-flavour non-universality*, *JHEP* **12** (2016) 059, [[1608.01349](#)].

[16] J. Kawamura, S. Okawa and Y. Omura, *Impact of the $b \rightarrow sll$ anomalies on dark matter physics*, [1706.04344](#).

[17] I. Garcia Garcia, *LHCb anomalies from a natural perspective*, *JHEP* **03** (2017) 040, [[1611.03507](#)].

[18] P. Ko, T. Nomura and H. Okada, *A flavor dependent gauge symmetry, Predictive radiative seesaw and LHCb anomalies*, [1701.05788](#).

[19] P. Ko, T. Nomura and H. Okada, *Explaining $B \rightarrow K^{(*)} \ell^+ \ell^-$ anomaly by radiatively induced coupling in $U(1)_{\mu-\tau}$ gauge symmetry*, *Phys. Rev. D* **95** (2017) 111701, [[1702.02699](#)].

[20] P. Ko, Y. Omura, Y. Shigekami and C. Yu, *LHCb anomaly and B physics in flavored Z models with flavored Higgs doublets*, *Phys. Rev. D* **95** (2017) 115040, [[1702.08666](#)].

[21] S. Di Chiara, A. Fowlie, S. Fraser, C. Marzo, L. Marzola, M. Raidal et al., *Minimal flavor-changing Z' models and muon $g - 2$ after the R_{K^*} measurement*, [1704.06200](#).

[22] R. Alonso, P. Cox, C. Han and T. T. Yanagida, *Anomaly-free local horizontal symmetry and anomaly-full rare B-decays*, [1704.08158](#).

[23] C. Bonilla, T. Modak, R. Srivastava and J. W. F. Valle, *$U(1)_{B_3-3L_\mu}$ gauge symmetry as the simplest description of $b \rightarrow s$ anomalies*, [1705.00915](#).

[24] J. Ellis, M. Fairbairn and P. Tunney, *Anomaly-Free Models for Flavour Anomalies*, [1705.03447](#).

[25] R. Alonso, P. Cox, C. Han and T. T. Yanagida, *Flavoured $B - L$ Local Symmetry and Anomalous Rare B Decays*, [1705.03858](#).

[26] Y. Tang and Y.-L. Wu, *Flavor Non-universality Gauge Interactions and Anomalies in B-Meson Decays*, [1705.05643](#).

[27] A. Datta, J. Kumar, J. Liao and D. Marfatia, *New light mediators for the R_K and R_{K^*} puzzles*, [1705.08423](#).

[28] C.-W. Chiang, X.-G. He, J. Tandean and X.-B. Yuan, $R_{K^{(*)}}$ and related $b \rightarrow s\ell\bar{\ell}$ anomalies in minimal flavor violation framework with Z' boson, [1706.02696](#).

[29] M. Bauer and M. Neubert, Minimal Leptoquark Explanation for the $R_{D^{(*)}}$, R_K , and $(g-2)_g$ Anomalies, *Phys. Rev. Lett.* **116** (2016) 141802, [\[1511.01900\]](#).

[30] D. Das, C. Hati, G. Kumar and N. Mahajan, Towards a unified explanation of $R_{D^{(*)}}$, R_K and $(g-2)_\mu$ anomalies in a left-right model with leptoquarks, *Phys. Rev. D* **94** (2016) 055034, [\[1605.06313\]](#).

[31] D. Bećirević, S. Fajfer, N. Košnik and O. Sumensari, Leptoquark model to explain the B -physics anomalies, R_K and R_D , *Phys. Rev. D* **94** (2016) 115021, [\[1608.08501\]](#).

[32] S. Sahoo, R. Mohanta and A. K. Giri, Explaining the R_K and $R_{D^{(*)}}$ anomalies with vector leptoquarks, *Phys. Rev. D* **95** (2017) 035027, [\[1609.04367\]](#).

[33] G. Hiller, D. Loose and K. Schönwald, Leptoquark Flavor Patterns & B Decay Anomalies, *JHEP* **12** (2016) 027, [\[1609.08895\]](#).

[34] B. Bhattacharya, A. Datta, J.-P. Guévin, D. London and R. Watanabe, Simultaneous Explanation of the R_K and $R_{D^{(*)}}$ Puzzles: a Model Analysis, *JHEP* **01** (2017) 015, [\[1609.09078\]](#).

[35] D. Bećirević and O. Sumensari, A leptoquark model to accommodate $R_K^{\text{exp}} < R_K^{\text{SM}}$ and $R_{K^*}^{\text{exp}} < R_{K^*}^{\text{SM}}$, [1704.05835](#).

[36] Y. Cai, J. Gargalionis, M. A. Schmidt and R. R. Volkas, Reconsidering the One Leptoquark solution: flavor anomalies and neutrino mass, [1704.05849](#).

[37] G. Bélanger, C. Delaunay and S. Westhoff, A Dark Matter Relic From Muon Anomalies, *Phys. Rev. D* **92** (2015) 055021, [\[1507.06660\]](#).

[38] B. Gripaios, M. Nardecchia and S. A. Renner, Linear flavour violation and anomalies in B physics, *JHEP* **06** (2016) 083, [\[1509.05020\]](#).

[39] Q.-Y. Hu, X.-Q. Li and Y.-D. Yang, $B^0 \rightarrow K^{*0}\mu^+\mu^-$ decay in the Aligned Two-Higgs-Doublet Model, *Eur. Phys. J. C* **77** (2017) 190, [\[1612.08867\]](#).

[40] G. D'Amico, M. Nardecchia, P. Panci, F. Sannino, A. Strumia, R. Torre et al., Flavour anomalies after the R_{K^*} measurement, [1704.05438](#).

[41] J. F. Kamenik, Y. Soreq and J. Zupan, Lepton flavor universality violation without new sources of quark flavor violation, [1704.06005](#).

[42] Z. Poh and S. Raby, Vector-like Leptons: Muon $g-2$ Anomaly, Lepton Flavor Violation, Higgs Decays, and Lepton Non-Universality, [1705.07007](#).

[43] S. Baek, N. G. Deshpande, X. G. He and P. Ko, Muon anomalous $g-2$ and gauged $L(\text{muon})$ - $L(\text{tau})$ models, *Phys. Rev. D* **64** (2001) 055006, [\[hep-ph/0104141\]](#).

[44] S. Baek and P. Ko, Phenomenology of $U(1)(L(\text{mu})-L(\text{tau}))$ charged dark matter at PAMELA and colliders, *JCAP* **0910** (2009) 011, [\[0811.1646\]](#).

[45] S. Baek, H. Okada and K. Yagyu, Flavour Dependent Gauged Radiative Neutrino Mass Model, *JHEP* **04** (2015) 049, [\[1501.01530\]](#).

[46] S. Baek, Dark matter and muon $(g-2)$ in local $U(1)_{L_\mu-L_\tau}$ -extended Ma Model, *Phys. Lett. B* **756** (2016) 1–5, [\[1510.02168\]](#).

[47] A. Crivellin, G. D'Ambrosio and J. Heeck, *Explaining $h \rightarrow \mu^\pm \tau^\mp$, $B \rightarrow K^* \mu^+ \mu^-$ and $B \rightarrow K \mu^+ \mu^- / B \rightarrow K e^+ e^-$ in a two-Higgs-doublet model with gauged $L_\mu - L_\tau$* , *Phys. Rev. Lett.* **114** (2015) 151801, [[1501.00993](#)].

[48] W. Altmannshofer and I. Yavin, *Predictions for lepton flavor universality violation in rare B decays in models with gauged $L_\mu - L_\tau$* , *Phys. Rev.* **D92** (2015) 075022, [[1508.07009](#)].

[49] P. Arnan, L. Hofer, F. Mescia and A. Crivellin, *Loop effects of heavy new scalars and fermions in $b \rightarrow s \mu^+ \mu^-$* , *JHEP* **04** (2017) 043, [[1608.07832](#)].

[50] S. Baek and Z.-F. Kang, *Naturally Large Radiative Lepton Flavor Violating Higgs Decay Mediated by Lepton-flavored Dark Matter*, *JHEP* **03** (2016) 106, [[1510.00100](#)].

[51] S. Baek, T. Nomura and H. Okada, *An explanation of one-loop induced $h \rightarrow E \bar{S} \bar{I} \bar{j} \bar{D}$ decay*, *Phys. Lett.* **B759** (2016) 91–98, [[1604.03738](#)].

[52] S. Baek, P. Ko and P. Wu, *Top-philic Scalar Dark Matter with a Vector-like Fermionic Top Partner*, *JHEP* **10** (2016) 117, [[1606.00072](#)].

[53] S. Baek, P. Ko and W.-I. Park, *Search for the Higgs portal to a singlet fermionic dark matter at the LHC*, *JHEP* **02** (2012) 047, [[1112.1847](#)].

[54] S. Baek, P. Ko, W.-I. Park and E. Senaha, *Higgs Portal Vector Dark Matter : Revisited*, *JHEP* **05** (2013) 036, [[1212.2131](#)].

[55] Y. Amhis et al., *Averages of b -hadron, c -hadron, and τ -lepton properties as of summer 2016*, [1612.07233](#).

[56] M. Misiak and M. Steinhauser, *Three loop matching of the dipole operators for $b \rightarrow s \gamma$ and $b \rightarrow s g$* , *Nucl. Phys.* **B683** (2004) 277–305, [[hep-ph/0401041](#)].

[57] G. Buchalla, A. J. Buras and M. E. Lautenbacher, *Weak decays beyond leading logarithms*, *Rev. Mod. Phys.* **68** (1996) 1125–1144, [[hep-ph/9512380](#)].

[58] PARTICLE DATA GROUP collaboration, C. Patrignani et al., *Review of Particle Physics*, *Chin. Phys.* **C40** (2016) 100001.

[59] UTfit collaboration, M. Bona et al., *The Unitarity Triangle Fit in the Standard Model and Hadronic Parameters from Lattice QCD: A Reappraisal after the Measurements of Delta $m(s)$ and $BR(B \rightarrow \tau \nu(\tau))$* , *JHEP* **10** (2006) 081, [[hep-ph/0606167](#)].

[60] J. Charles et al., *Current status of the Standard Model CKM fit and constraints on $\Delta F = 2$ New Physics*, *Phys. Rev.* **D91** (2015) 073007, [[1501.05013](#)].

[61] T. Jubb, M. Kirk, A. Lenz and G. Tetlalmatzi-Xolocotzi, *On the ultimate precision of meson mixing observables*, *Nucl. Phys.* **B915** (2017) 431–453, [[1603.07770](#)].

[62] G. Bélanger, F. Boudjema, A. Pukhov and A. Semenov, *microOMEGAs4.1: two dark matter candidates*, *Comput. Phys. Commun.* **192** (2015) 322–329, [[1407.6129](#)].